

Effect of electromagnetic waves and higher harmonics in capacitively coupled plasma phenomena

This content has been downloaded from IOPscience. Please scroll down to see the full text.

2013 J. Phys. D: Appl. Phys. 46 472001

(<http://iopscience.iop.org/0022-3727/46/47/472001>)

View [the table of contents for this issue](#), or go to the [journal homepage](#) for more

Download details:

IP Address: 128.83.63.20

This content was downloaded on 05/11/2013 at 15:00

Please note that [terms and conditions apply](#).

FAST TRACK COMMUNICATION

Effect of electromagnetic waves and higher harmonics in capacitively coupled plasma phenomena

R R Upadhyay¹, I Sawada², P L G Ventzek³ and L L Raja⁴¹ Esgee Technologies Inc., 1301S. Capital of Texas Hwy., Austin, TX 78746, USA² Tokyo Electron U.S. Holdings, Inc., 2400 Grove Boulevard, Austin, TX 78741, USA³ Tokyo Electron America, Inc., 2400 Grove Boulevard, Austin, TX 78741, USA⁴ Department of Aerospace Engineering and Engineering Mechanics, The University of Texas at Austin, 1 University Station, Austin, TX 78712, USA

Received 31 August 2013, in final form 10 October 2013

Published 5 November 2013

Online at stacks.iop.org/JPhysD/46/472001**Abstract**

High-resolution self-consistent numerical simulation of electromagnetic wave phenomena in an axisymmetric capacitively coupled plasma reactor is reported. A prominent centre-peaked plasma density profile is observed for driving frequencies of 60 MHz and is consistent with observations in the literature and accompanying experimental studies. A power spectrum of the simulated wave electric field reveals the presence of well-resolved high frequency harmonic content up to the 20th harmonic of the excitation frequency; an observation that has also been reported in experiments. Importantly, the simulation results reveal that the occurrence of higher harmonics is strongly correlated with the occurrence of a centre-peaked plasma density profile.

(Some figures may appear in colour only in the online journal)

Very-high-frequency (VHF) operation (30 MHz and higher) of capacitively coupled plasma (CCP) reactors in semiconductor and flat panel manufacturing have the advantage of generating high plasma densities at low input powers and low plasma potential. However, high-frequency operation is accompanied by a non-uniform centre-peaked plasma density distribution over the processing surface, generally attributed to electromagnetic (EM) wave effects in the reactor [1]. These effects are believed to result from EM standing waves whose plasma-reduced quarter wavelengths can approach the wafer radius ($\lambda/4 \approx 10$ cm for frequencies approaching 200 MHz) [1–3]. Indeed, as both the CCP operational frequencies and wafer areas become larger, these effects become more pronounced.

Our present understanding of EM wave effects in VHF-CCP reactors is focused on the fundamental excitation frequency, its standing wave in the reactor, and the corresponding influence on the plasma uniformity. However, a straightforward analysis of standing wave effects at

the fundamental excitation frequency does not explain the observation of a sharp centre-peaked profile in semiconductor processing reactors with wafer radius of ~ 10 cm driven at a frequency of 60 MHz. For example, the plasma-reduced quarter wavelength at 60 MHz is about 40 cm which is significantly greater than the wafer radius. Experimental studies of higher harmonic wave content of the fundamental excitation frequency in these reactors provide a plausible explanation. For example, studies by Miller *et al* [4] used a *B-dot* probe in the plasma and report up to the 10th harmonics of the EM wave for a fundamental 60 MHz excitation, i.e. relatively strong EM wave content up to 600 MHz was measured. The authors attributed the existence of higher harmonics to the complex interactions between the external circuit driving the reactor and the non-linear sheaths. Certainly, the 3rd harmonic and higher for the 60 MHz fundamental produce a standing wave with quarter wavelength smaller than the wafer radius and can explain the strong centre-peak plasma density profile in the reactor. If indeed the higher harmonics

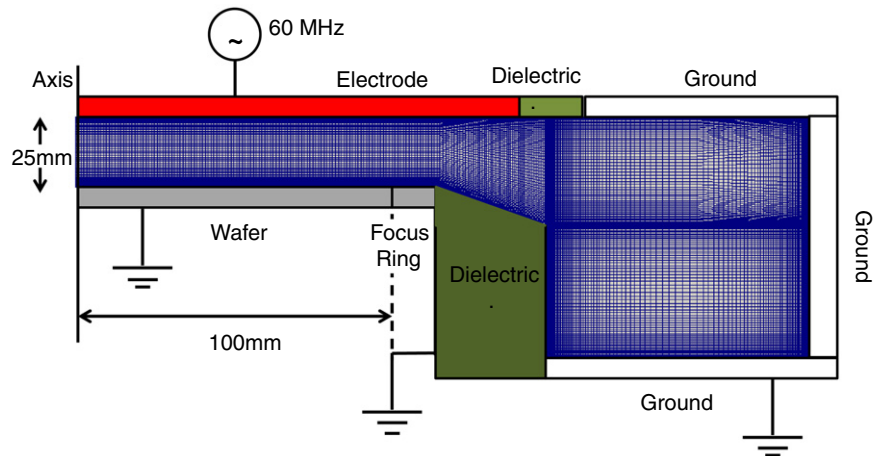


Figure 1. Schematic of capacitively coupled reactor and the high-resolution computational mesh for the simulations.

of the EM wave (10th harmonic and higher for a 60 MHz fundamental) were important, then it would stand to reason that fine structure of the wave field in the reactor would be important and must be resolved carefully in any study of EM wave effects in VHF-CCP reactors. For example, at 600 MHz the plasma-reduced wavelength is about 2 cm [2] and hence it is necessary to spatially and temporally resolve fine structures present at this scale.

Several recent computational studies of EM wave effects in VHF-CCP reactors have been reported. Of these, the models that provide a full physics representation of EM wave phenomena in the plasma [5–7] report self-consistent predictions of the centre-peaked profile. These reports do not, however, discuss the higher harmonic content of EM waves in the plasma and whether their computational model provided adequate spatio-temporal resolution to resolve these higher harmonic EM wave contents.

In this work we develop a high-resolution, first-principles computational model of the coupled plasma-EM wave phenomena. Results from an accompanying experimental study in a VHF-CCP reactor is used to show the sharp nature of the centre-peaked plasma density profiles in these systems. Simulation results for the electron density profiles, plasma power deposition and the fast Fourier transform (FFT) of the electric field signal at the axial mid-gap location are reported. A comparison of these quantities is made with simulation results where the EM wave phenomenon is excluded from the plasma model. The FFT of the time series of computed EM wave field shows clear existence of higher harmonic waves up to the time resolution of the computational method. Importantly, the strong correlation between the occurrence of a centre-peak plasma profile and the existence of the higher harmonics is also reported.

Figure 1 shows a schematic of the capacitively coupled reactor along with the computational mesh used in the simulations. The axisymmetric reactor chamber is driven by a top electrode of conductive silicon that sits parallel to a bottom grounded (process) surface of 100 mm radius. The inter-electrode gap between the powered electrode and the grounded surface is 25 mm. The remaining part of the reactor comprises the pump-port region that is enclosed by grounded

walls with quartz dielectric breaks. The top powered electrode, modelled as a dielectric, is connected to a voltage source. The computational mesh comprises a total of 25 025 cells with cells that are gradually clustered towards the metal and dielectric surfaces that bound the plasma. The smallest cell sizes at the wall boundaries are about $100\ \mu\text{m}$ and are comparable to the plasma Debye length. Independent mesh resolution studies, suggest that this level of resolution is necessary to adequately resolve all the fine scale features such as the higher harmonic EM wave content in the plasma, the EM wave skin depths, and the localized electrostatic Joule heating in the sheath edge regions of the plasma. Simulations with coarser meshes are found to have several undesirable effects such as spurious plasma discharges, unphysical space charge fluctuations due to inadequate resolution of the sheaths and other numerical artefacts. For the operating conditions, we assume a 60 MHz sinusoidal voltage (with magnitude adjusted to achieve a set power of 1000 W) applied to the top powered electrode. A pure argon plasma at a pressure of 100 mTorr (13 Pa) is used.

We use a multi-species, two-temperature fluid description of the plasma whereby equations for individual species number density conservation (ions, electrons and neutral), momentum equations for ions, and the electron energy conservation are solved simultaneously [8]. The gas-phase plasma reaction mechanism for argon and the formulation for the species transport properties are the same as in [9] with the exception that the rate coefficients for electron-impact reactions and electron transport properties are calculated using an off-line Boltzmann equation solver [10] for an excitation frequency of 60 MHz. Maxwell's equations for EM wave phenomena in the reactor are solved using the time-dependent magnetic vector potential approach with the Coulomb gauge. The solution is entirely self-consistent in that the space charge and plasma currents that are source terms for Maxwell's equation are obtained from the plasma simulations and the computed electric fields are fed back to the plasma simulations to compute the transport and Joule heating of charged particles. We note that the simulations with plasma equations coupled to the time-dependent wave equations are computationally demanding due to a minimum Courant–Friedrichs–Lewy criterion for the wave equation. For the minimal grid

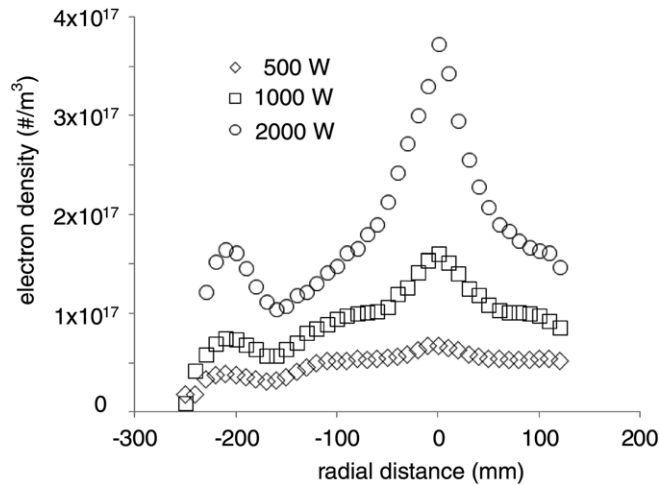


Figure 2. Experimentally measured electron density profiles along the reactor mid-gap for 100 mTorr argon plasma.

sizes that we use, the time steps for wave equation are of the order of 10^{-13} s. For tractable simulations, a sub-cycling approach, where wave equation is solved with a much smaller time step while freezing the plasma variables, is used. Use of approximations such as quasi-electrostatics or the Darwin approximation [11] could reduce computing times significantly, but these approximations either truncate the high-frequency EM wave components or eliminate the speed of light entirely, and hence do not represent the entire range of frequencies that are relevant to the EM wave phenomena in this study.

Experiments were performed in a non-commercial test bench reactor system with a geometry similar to that shown in the schematic in figure 1. Figure 2 shows the experimentally measured radial profiles of the electron number density along the mid-gap between the two parallel electrodes. The point measurements of the plasma electron density were performed using a plasma absorption probe (PAP) [12]. The measurements were made at 60 MHz driving frequency, 100 mTorr pressure and powers ranging from 500 to 2000 W. Repeated measurements in similar setups have shown that the experimental errors in the density are within $\pm 10\%$. Notable features of the electron density profiles are an overall increase in the electron densities with increasing powers and the formation of a strong and sharp centre-peak profile for powers exceeding 500 W. The sharp centre peak is indicative of a narrowly confined plasma generation process taking place on a radial length scale of a few centimetres along the axis of the reactor. As noted earlier, such a small length scale is inconsistent with the plasma-reduced quarter wavelength for the 60 MHz fundamental excitation, but is possibly described by the plasma-reduced quarter wavelength for higher harmonics of the fundamental. As noted earlier, frequencies around the 10th harmonic (600 MHz) has a plasma-reduced quarter wavelength that is comparable with the radial extent of the sharp centre-peak plasma density profile. Another feature of the experimental profiles is the occurrence of a secondary peak in the outer (pump-port) region of the reactor that increases with increasing power.

The simulation results reported here are for 1000 W. To clearly establish the importance of the EM waves and the higher harmonic frequency content of the wave, two simulations were performed, one with the coupled plasma-EM wave governing equations ('coupled plasma-EM wave') and the other with only the plasma-electrostatic field equations ('plasma-electrostatic only'). Simulation results for the cycle-averaged electron number density for the two cases are shown in figure 3. The plasma-electrostatic only results show the peak electron density is off-centre (axis) at a mid-gap location roughly coinciding with the breakpoint between the lower grounded electrode and the dielectric. For the coupled plasma-EM wave case, the peak electron density is located mid-gap at the centre (axis) of the reactor. These results are well-known in the literature. For example in [1], it is argued that purely electrostatic edge effects are responsible for causing an off-centre peak, while EM standing wave effects diminish the edge peak and promote the growth of a centre peak. Our simulation results support this general hypothesis.

As noted earlier, the centre-peaked electron density distribution in a VHF-CCP is widely explained by invoking the concept of the EM standing wave phenomena. The standing wave pattern causes constructive interference of the waves leading to an enhanced value of the field at the centre axis and, therefore, larger power deposition and production of electrons in that region. The standing wave effect is, however, expected to decrease with increasing power (and hence increasing number density of electrons) due to the skin effect [1]. The skin effect is believed to cause shielding of the waves in the plasma bulk and higher power deposition at the edges of the electrodes leading to an edge peaked electron density profile. This picture is at odds with our experimental measurements shown in figure 2 that actually shows increasingly sharp centre peak in electron density with increasing power. In figure 4, we plot the electron power absorption due to the electrostatic Joule heating in the plasma-electrostatics only simulation and EM wave heating in the coupled plasma-EM wave simulation. The electrostatic Joule heating in the coupled plasma-EM wave case is qualitatively and quantitatively similar to the plasma-electrostatic only case. The electron power absorption due to the electrostatic field is largest near the edge of the sheath. In contrast, the electron power absorption due to the EM field, is significant in the axial mid-gap region. In the coupled plasma-EM wave case, the maximum power deposition due to the electrostatic component is around an order of magnitude higher than the EM wave heating, although the latter is spread out over a much larger volumetric region of the inter-electrode gap. In figure 5, we show the results of an FFT of the axial component of the electrostatic field in the plasma-electrostatic only case and the EM wave field in the coupled plasma-EM wave case. For the plasma-electrostatic only case, we see that the spectrum consists of predominantly the 60 MHz driving fundamental frequency. However, for the coupled plasma-EM wave case, we see that in addition to the fundamental driving frequency there is a strong presence of the higher harmonics; the 9th harmonic being particularly prominent. The higher harmonic components of the wave are more efficient in power deposition. For the maximum value of

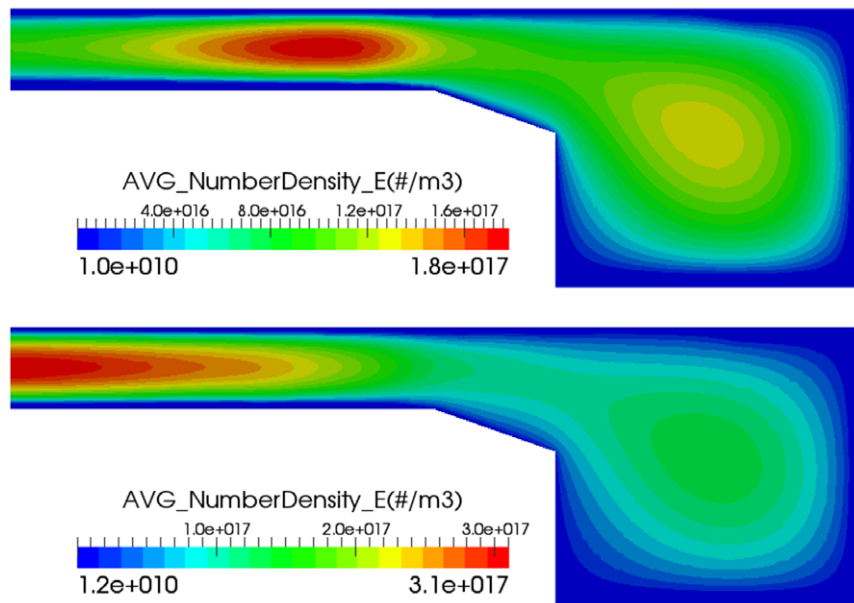


Figure 3. Computational results for the electron density in the reactor for 100 mTorr argon discharge driven at 60 MHz. Top: plasma-electrostatics only. Bottom: coupled plasma-EM wave.

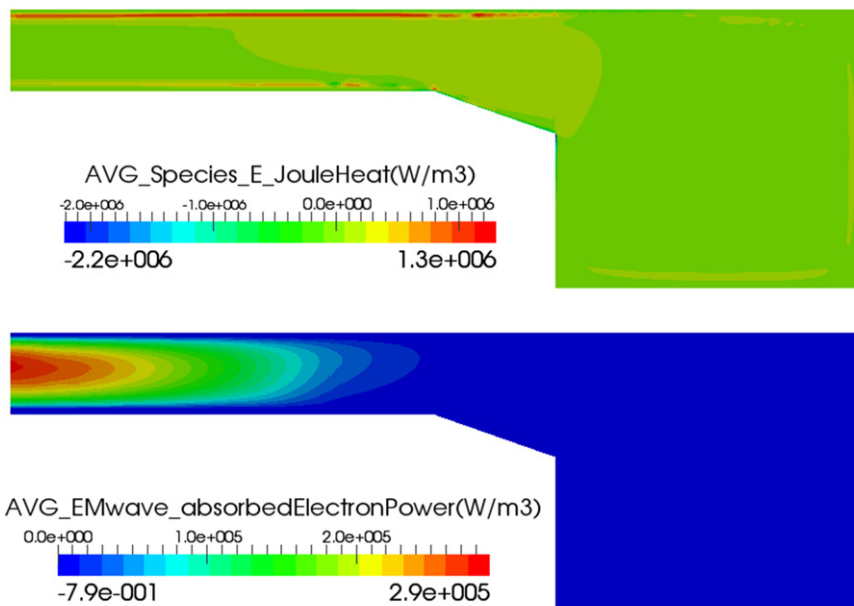


Figure 4. Computational results for the electron power deposition in the reactor for 100 mTorr argon discharge driven at 60 MHz. Top: electrostatic Joule heating in the plasma-electrostatics only case. Bottom: EM power deposition in the coupled plasma-EM wave case.

the number density of $\sim 3 \times 10^{17} \text{ # m}^{-3}$ from figure 3, the wave cutoff frequency (corresponding to the plasma frequency) is roughly 5 GHz, indicating that most of the waves in our FFT are evanescent. Our findings are consistent with the experimental results presented in [4] that showed the existence of higher harmonics in the plasma bulk, especially in the centre mid-gap between the electrodes. The presence of these waves could be due to the larger skin depths near the sheath edge. For example using the skin depth expression given in [13], with appropriate parameters typical in our simulations, we see that the skin depth varies from 17.5 to 19 mm as the frequency varies from 60 MHz to 1.2 GHz. Although evanescent waves are strongly attenuated, we will still find EM waves of the

fundamental driving frequency and their higher harmonics in the bulk plasma. This seems to suggest that evanescent waves play a key role in electron power deposition. Although not conclusive, this is strong evidence that the higher harmonics of the EM wave field play a crucial role in determining the plasma density profile throughout the reactor and that the control or suppression of these harmonics is essential to achieve high uniformity that is desirable for etch and deposition applications.

While both numerical simulations and experimental measurements reveal the presence of the higher harmonics, the mechanisms by which they are generated and selectively amplified are not very well understood. As higher harmonics

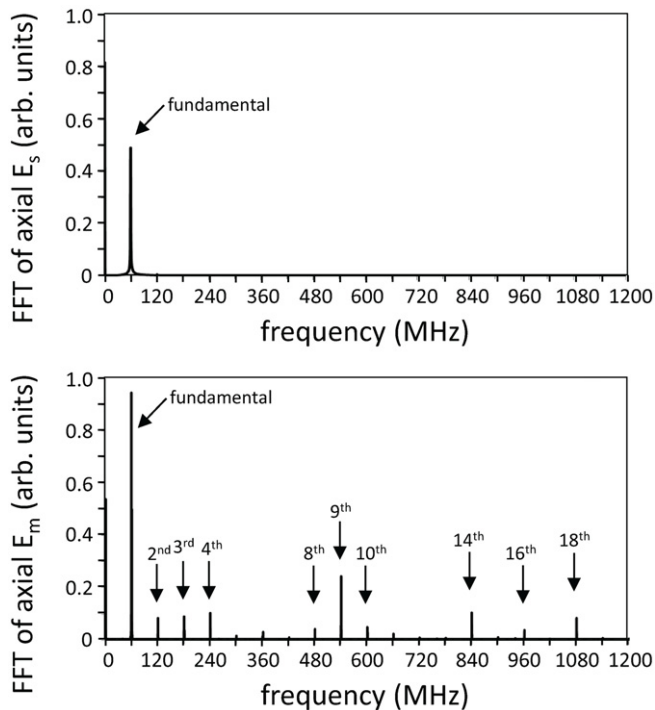


Figure 5. FFT of the axial electric fields in the mid-gap axial location of the reactor for 100 mTorr argon discharge driven at 60 MHz. Top: FFT of the electrostatic field in the plasma-electrostatics only. Bottom: FFT of the EM field in the coupled plasma-EM wave case.

appear to strongly influence plasma uniformity, use of sufficiently small spatial grids and time steps for their resolution in computer simulations is essential. Previous studies have mentioned the phenomena of plasma series resonance (PSR) [14, 15] that can amplify certain harmonics of the plasma current. By looking at the FFT of the circuit current, we did not see direct evidence of PSR in our simulations.

In summary, computational simulation of EM wave phenomenon in a VHF-CCP reactor, with resolution of all the important spatial and temporal scales, is presented. The computational model results show non-uniformity in the plasma density profile, as also seen in experimental

observations. FFT of the time series of computed EM wave field shows clear existence of a series of higher harmonics. Importantly, the strong correlation between the occurrence of a centre-peak plasma profile and the existence of the higher harmonics is reported.

Acknowledgment

The authors express their gratitude to T Ohshita and M Vukovic who have provided valuable advice and support.

References

- [1] Lee I, Graves D B and Lieberman M A 2008 *Plasma Sources Sci. Technol.* **17** 015018
- [2] Chabert P, Raïmbault J-M, Levif P, Rax R-M and Lieberman M A 2005 *Plasma Sources Sci. Technol.* **15** S130
- [3] Song D, Jeong S, Park Y, Volynets V N, Ushakov A G and Kim G-H 2009 *J. Vac. Sci. Technol. A* **27** 13–19
- [4] Miller P A, Barnat E V, Hebner G A, Paterson P A and Holland J P 2006 *Plasma Sources Sci. Technol.* **15** 889–99
- [5] Yang Y and Kushner M J 2010 *J. Appl. Phys.* **108** 113306
- [6] Chen Z, Rauf S and Collins K 2010 *J. Appl. Phys.* **108** 073301
- [7] Zhang Y-R, Xu X, Bogaerts A and Wang Y-N 2012 *J. Phys. D: Appl. Phys.* **45** 015202
- [8] 2013 *VizGlow: Plasma Modeling Software for Multi-Dimensional Simulations of Non-Equilibrium Glow Discharge Systems* Theory Manual, version 1.9 (Austin, TX: Esgee Technologies Inc.)
- [9] Raja L L, Mahadevan S, Ventzek P L G and Yoshikawa J 2013 *J. Vac. Sci. Technol. A* **31** 031304
- [10] Hagelaar G J M and Pitchford L G 2005 *Plasma Sources Sci. Technol.* **14** 722–33
- [11] Eremin D, Hemke T, Brinkmann R P and Mussenbrock T 2013 *J. Phys. D: Appl. Phys.* **46** 084017
- [12] Kokura H, Nakamura K, Ghanashev I P and Sugai H 1999 *Japan. J. Appl. Phys.* **38** 5262–6
- [13] Makabe T and Petrovic Z 2006 *Plasma Electronics: Applications in Microelectronic Device Fabrication* (Boca Raton, FL: CRC Press) pp 284–6
- [14] Lieberman M A, Lichtenberg A J, Kawamura E, Mussenbrock T and Brinkmann R P 2008 *Phys. Plasmas* **15** 063505
- [15] Yamazawa Y 2009 *Appl. Phys. Lett.* **95** 191504